

## Structure and electronic properties of thin Ge<sub>2</sub>Sb<sub>2</sub>Te<sub>5</sub> films produced by DC ion-plasma sputtering

S. Sultanbekov<sup>a</sup>, O. Prikhodko<sup>b</sup>, N. Almas<sup>c,\*</sup>

<sup>a</sup>*Volkovgeology JSC, Kazatomprom, 168, Bogenbai batyr Street, Almaty, Kazakhstan, 050012*

<sup>b</sup>*IETP, NAO Al-Farabi Kazakh National University, 71 Al-Farabi Avn, 050040, Almaty, Kazakhstan*

<sup>c</sup>*Department of Science and Innovation, Astana IT University, Mangilik Yel, 55/11, Astana, Kazakhstan, 010000*

The optical properties of Ge<sub>2</sub>Sb<sub>2</sub>Te<sub>5</sub> thin films were studied as a function of thickness. An increase in optical band gap with decreasing film thickness has been observed. The current–voltage characteristics measured in Ge<sub>2</sub>Sb<sub>2</sub>Te<sub>5</sub> thin films in the current mode are studied. A decrease in switching time and threshold voltage with decreasing film thickness is established.

(Received April 13, 2023; Accepted July 17, 2023)

*Keywords:* Chalcogenide glassy semiconductors, Switching effect, PC-RAM, Atomic structure, Electronic properties

### 1. Introduction

A broad class of non-crystalline materials is the chalcogenide glassy semiconductors (CGS) family. These substances are known as chalcogen materials because they contain chalcogen atoms like Se, S, or Te in their composition. These chalcogens form various compounds with elements of the fifth (As, Sb, etc.) or fourth (Si, Ge, etc.) groups. These include two-, three- and multicomponent glassy alloys of chalcogenides (sulfides, selenides, and tellurides) of various metals (for example, Ge-S, As-S, Ge-Se, As-Se, Ge-As-Se, As-S -Se, As-Ge-Se-Te, Ge-S-Se, As-Sb-S-Se, Ge-Sb-Te, etc.). In the 1955s, researchers from the Ioffe Physico-Technical Institute, Goryunova N.A., and Kolomeyts B.T., revealed semiconducting properties of chalcogenide glasses [1,2]. Following extensive research, a "switching effect" in chalcogenide glassy semiconductors was discovered, consisting of an abrupt and reversible phase transition from the glassy to the crystalline state. In 1968, it was patented [3]. Immediately after the discovery of CGS, researchers faced the question of modifying these materials with impurities. And until the 1970s, attempts to introduce an impurity into the CGS matrix did not lead to the proper result. This situation persisted until the 1970s, and it was believed that impurities do not affect the properties of CGS. Further, Mott established a fundamental position about the inactivity of dopants on the properties of CGS "8-N", where N is the number of valence electrons of the doping atom, and 8 - N is the number of its valence bonds. According to this statement, all impurity atoms in a disordered CGS matrix can saturate their valence bonds without creating donor–acceptor levels, and therefore doping was impossible [4,5]. However, it was believed that the modification makes it possible to improve the electrical properties of CGS. An increase in conductivity in silver-modified As<sub>2</sub>Se<sub>3</sub> films was reported in Ref. 6, which confirmed the possibility of modifying the CGS matrix with metals. At the same time, Anderson introduced a hypothesis in which it is said that there are intrinsic structural defects in CGS that fix the Fermi level in the middle of the band gap, the so-called U-centers, centers with negative correlation energy. In 1987, Yamada et al. [7] found that the Ge-Sb-Te compound, lying on the line of the quasi-binary cut Sb<sub>2</sub>Te<sub>3</sub> - GeTe, has a fast crystallization process, which served as an impetus for the development of optical storage media such as (DVD, Blu-Ray). In 1999, Ovonics patented a memory

---

\* Corresponding author: n.almas@astanait.edu.kz  
<https://doi.org/10.15251/CL.2023.207.487>

based on the phase change of CGS, and only 10 years after the creation of the first optical media based on CGS, in 2011, Samsung released the first industrial product in its phone with a memory capacity of 512 MB, using an electric impulse in as a phase switch. But the still large-scale use of CGS-based memory elements is the subject of numerous studies, since the stability and improvement of parameters by searching for the right material with desired properties remains one of the factors hindering mass production.

The atomic structure of the composition  $\text{Ge}_2\text{Sb}_2\text{Te}_5$  consists of two binary compounds Ge-Te and Sb-Te. The structure of the  $\text{Ge}_2\text{Sb}_2\text{Te}_5$  composition is characterized by three states "glassy - cubic crystalline - hexagonal crystalline", and its change is achieved by heating to a certain temperature of phase transitions. As reported in [8], Ge atoms can occupy a tetrahedral, pyramidal, or distorted octahedral coordination position in the  $\text{Ge}_2\text{Sb}_2\text{Te}_5$  matrix. The position of the germanium atom has various spatial variations, differing in bond lengths. During the transition from an amorphous structure to an intermediate cubic crystalline state, the Ge atom is rearranged from tetrahedral to octahedral coordination. The intermediate crystalline cubic structure of  $\text{Ge}_2\text{Sb}_2\text{Te}_5$  is an fcc cell of the sodium chloride type NaCl (Fig. 1), with the formation of vacancies occupying 20% of the cell. The presence of a vacancy in such a structure indicates that Ge and Sb do not have enough valence electrons to form a bond in the lattice [9]. Such a transition occurs when the temperature reaches 100–170° C. As the temperature rises above 270°C, a phase transition occurs from fcc to a hexagonal stable crystalline structure, which consists of alternating hexagonal layers arranged in the order Te-Sb-Te-Ge-Te-Te-Ge-Te-Sb-Te. Using X-ray absorption extended fine structure spectroscopy for the  $\text{Ge}_2\text{Sb}_2\text{Te}_5$  crystalline hexagonal structure, it was found that upon transition to a stable crystalline state, the material has rigid short covalent bonds of Ge-Te atoms (2.83 and 3.2 Å) and weak elongated bonds between Sb-Te atoms (2.91 and 3.2 Å) [10]. In addition, it was found that the local  $\text{Ge}_2\text{Sb}_2\text{Te}_5$  structure is determined by Te atoms forming a stable sublattice.

Chalcogenide glassy semiconductors based on the quasi-binary GeTe-Sb<sub>2</sub>Te<sub>3</sub> have found their wide application in optical information recording devices (DVD, Blue-Ray) based on the reversible glass-to-crystal phase transition. The principle of operation in optical information carriers is based on the reflection of laser radiation from two different phase states, that is, different reflectance values for the amorphous and crystalline phases correspond to different reflection values, where information is written as a logical zero and one for two phase states. In memory cells of the new generation of the PCM type, the principle of operation is based on a similar phase transition, only when exposed to a current pulse. And the generally accepted definition is that the switching effect is a reversible phase transition of a material from a high-resistance state (off-state) to a low-resistance state (on-state) under the action of an electrical impulse, in a short period of time ~ 100 ns upon reaching a certain threshold voltage  $U_{th}$  (threshold voltage) [13].

Such a transition is characterized by the presence of an abrupt increase in the conductivity by several orders of magnitude and a decrease in resistivity from ~  $10^5$  to 1 Ohm\*cm. With the switching effect on the volt-ampere characteristics, a section with negative differential resistance is observed, characteristic of materials, where the so-called electrical breakdown occurs with the formation of a current filament. Current lacing is observed in strong electric fields (~  $10^5$  V/cm), where the I-V characteristic deviates from Ohm's law, and its form takes an S-shape. The current density in the filament is many times greater than in the surrounding volume, and it flows mainly inside the filament, even though the cross section of such a filament is many times smaller than the transverse size of the sample.

Despite the apparent simplicity of the switching and memory effect, the physics of the process is still the subject of research and discussion. To explain this phenomenon in CGS, several models based on the electronic, thermal, or electron-thermal nature of the phenomena were proposed.

## 2. Experimental part

### 2.1. Thin film synthesis

The preparation of Ge<sub>2</sub>Sb<sub>2</sub>Te<sub>5</sub> films was carried out by the method of ion-plasma magnetron sputtering of a monolithic polycrystalline target of Ge<sub>2</sub>Sb<sub>2</sub>Te<sub>5</sub> composition with a chemical purity of 99.999% from AciAlloys (USA). Films were obtained in an argon atmosphere at a pressure of ~1 Pa. The accelerating voltage was 400 V, the film deposition rate was ≈0.3 nm/s. Films were deposited on substrates at room temperature. Quartz, single-crystal silicon, and Kapton polyimide films were used as substrates, which were preliminarily subjected to chemical and thermal treatment. Bismuth-modified Ge<sub>2</sub>Sb<sub>2</sub>Te<sub>5</sub> films were obtained by ion-plasma co-sputtering of a combined target. Pieces of bismuth were evenly placed on a CGS target in the sputtering zone. The change in the bismuth impurity concentration in the films was achieved by varying the ratio of the surface areas of the metal and CGS targets. The purity of bismuth was 99.999%.

### 2.2. Thin film characterization and measurements

The elemental composition and morphology of thin films were measured by energy dispersive analysis (EDXS) and scanning electron microscopy using Quanta 3D 200i complex. The electron beam energy was 30 keV. The film thickness was determined by scanning a cleavage of a Ge<sub>2</sub>Sb<sub>2</sub>Te<sub>5</sub> film deposited on crystalline silicon.

The structure of the films was studied using high-resolution transmission electron microscopy. The measurements were carried out on a Fei Titan electron microscope with a polyemission cold cathode (Field Emission Cathode) and a hexapole image corrector (CEOS corrector). The TEM resolution was about 0.1 nm, the applied voltage was 300 kV, and the beam current was 2 nA.

Optical transmission  $T(\lambda)$  and reflection  $R(\lambda)$  spectra of Ge<sub>2</sub>Sb<sub>2</sub>Te<sub>5</sub> films were recorded at room temperature in the wavelength range from 300 to 2000 nm on a Shimadzu UV3600 spectrophotometer.

To study the electrical properties, the samples were prepared with a planar arrangement of electrodes with a gap of 100 μm on a Kapton polyimide film with a specific resistance of ~10<sup>17</sup> Ω cm. The temperature dependences of the electrical conductivity of CGS films were studied using a Keithley-6485 picoammeter in the temperature range from 300 to 400 K at direct current at an electric field strength of 10<sup>2</sup> V/cm in the region of linearity of the current-voltage characteristic (CVC) of the samples. The sample heating rate was 2°/min. The sample temperature was recorded with a copper-constantan thermocouple.

The errors of the main semiconductor parameters of the studied films were determined by the spread of their values from sample to sample and amounted to conductivity ( $\Delta\sigma$ ) half an order of magnitude, for the activation energy of conductivity ( $\Delta E\sigma$ ) and the optical band gap ( $\Delta E_g$ ) ±0.02 eV and ±0.01 eV, respectively.

## 3. Results and discussion

### 3.1. EDXS

A typical EDX spectrum and surface morphology of a sample is shown in Figure 1. The surface of the films was homogeneous. Table 1 shows the resulting EDX values. The films do not contain contaminants. The estimated elemental ratio showed that the measured and selected values were in good agreement. The results of film thickness measurements are shown on Figure 2.

Table 1. Elemental composition of Ge<sub>2</sub>Sb<sub>2</sub>Te<sub>5</sub> film.

Element	Ge	Sb	Te
Wt%	14,66	23,65	61,70
At%	22,95	22,08	54,97
Wt% - weight percent, At% - atomic percent			

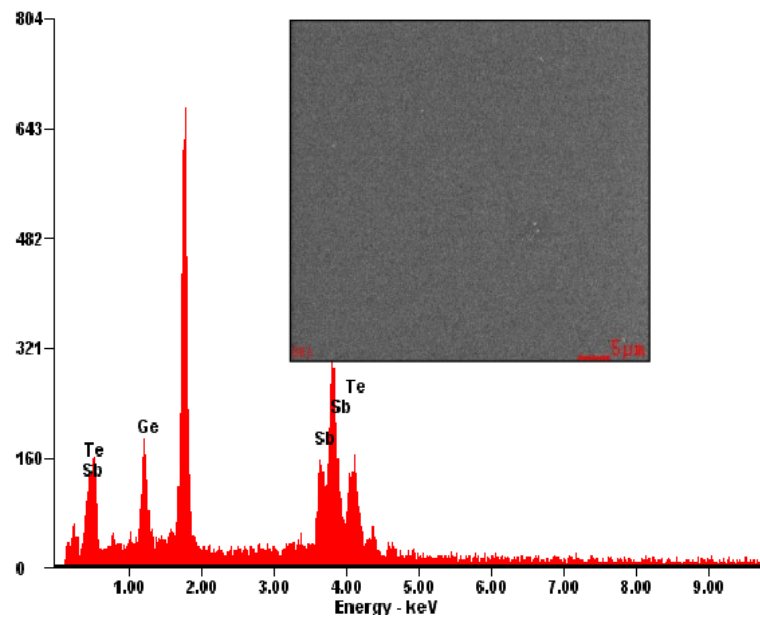


Fig. 1. Typical EDX spectra and morphology (onset) of  $\text{Ge}_2\text{Sb}_2\text{Te}_5$  film.

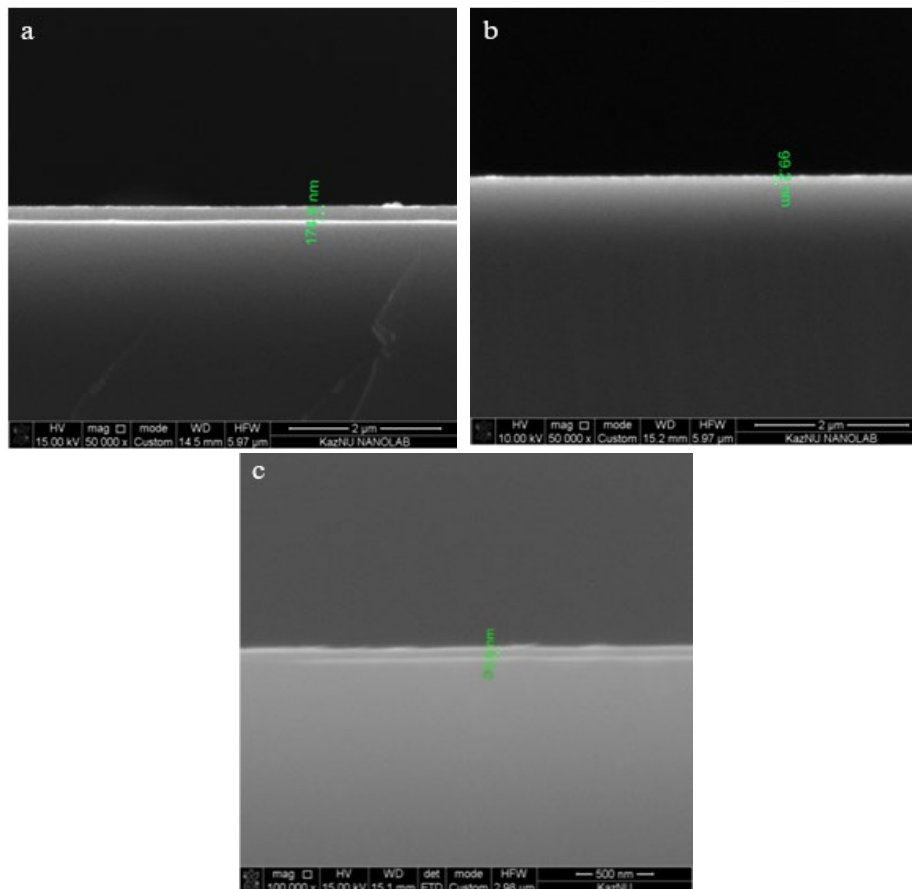


Fig. 2. SEM images of cleaved  $\text{c-Si} - \text{Ge}_2\text{Sb}_2\text{Te}_5$  film: a) ~175 nm; b) ~100 nm; c) ~50 nm.

### 3.2. TEM

The structure of the films was studied using high-resolution transmission electron microscopy (TEM-HR). HR-TEM was carried out on a Fei Titan electron microscope with a polyemission cold cathode (Field Emission Cathode) and a hexapole image corrector (CEOS corrector). The TEM resolution was  $<0.1$  nm, the applied voltage was 300 kV, and the beam current was several nA. The results of transmission electron microscopy are shown in Fig. 3.

It has been established that the films are continuous and have a typical amorphous structure with a short-range order, which is quite clearly visible on microphotographs with a resolution of 5 nm (Fig.3 (c)). The electron diffraction pattern clearly shows diffuse diffraction rings characteristic of an amorphous structure (Fig. 3 (d)).

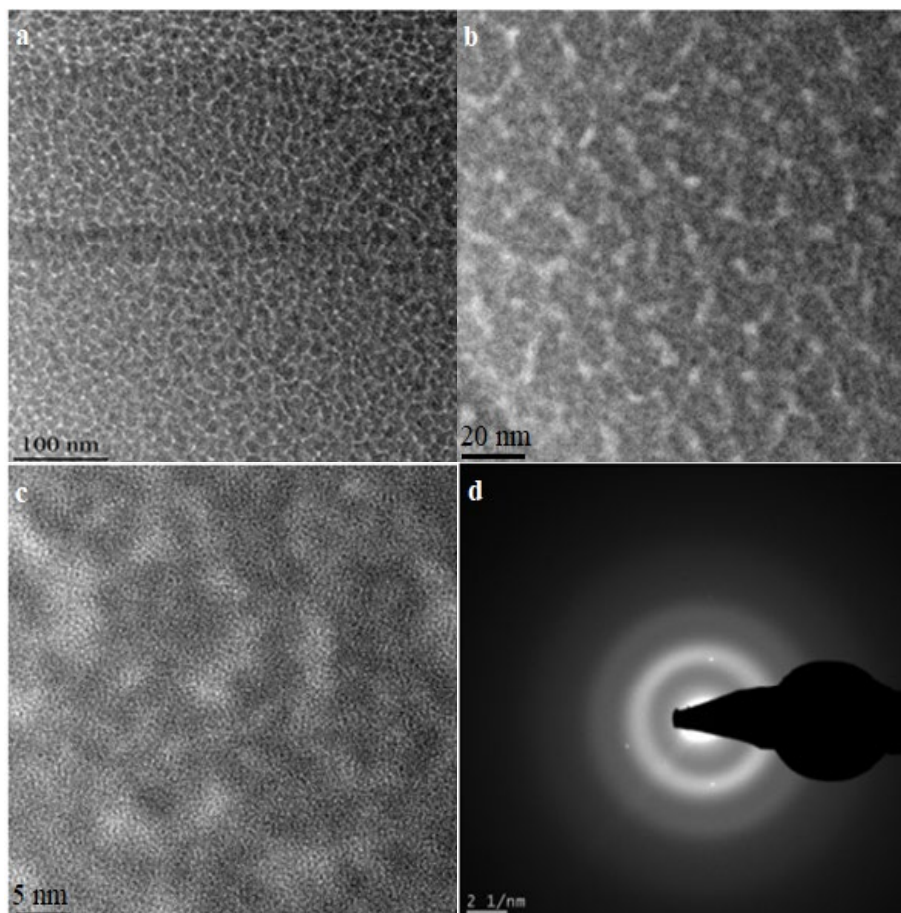


Fig. 3. TEM images of  $Ge_2Sb_2Te_5$  films with a resolution of 100 nm (a), 20 nm (b), 5 nm (c) and an electron diffraction pattern (d).

### 3.3. Optical properties of thin films

Optical transmission spectra  $T(\lambda)$  and reflectance  $R(\lambda)$  of  $Ge_2Sb_2Te_5$  films shown in Fig. 4. All spectra were recorded at room temperature in the wavelength range from 300 to 2000 nm on a Shimadzu UV3600 spectrophotometer.

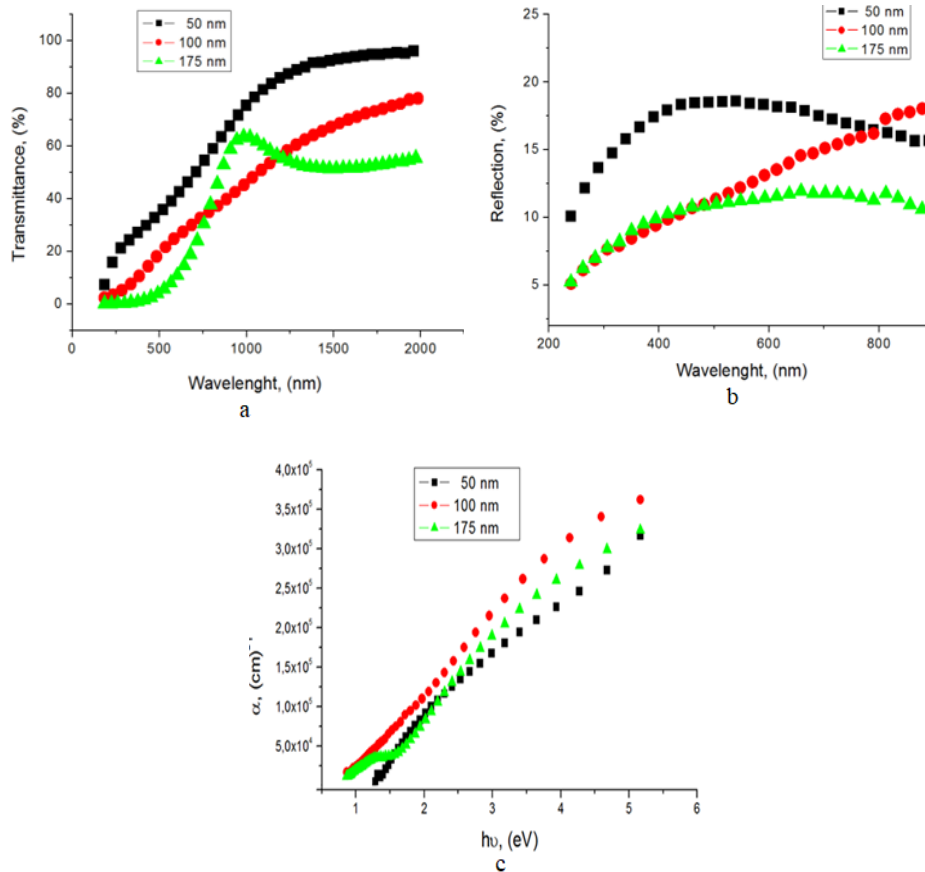


Fig. 4. Optical transmission (a), reflection (b), and absorption (c) spectra of  $Ge_2Sb_2Te_5$  films.

With known values of sample thickness  $l$ , transmission coefficients  $T(\lambda)$  and reflection  $R(\lambda)$  of light, the absorption coefficient  $\alpha$  was determined:

$$\alpha(\lambda) = (1/l) \cdot \ln \{ T(\lambda) / (1 - R(\lambda)^2) \} \quad (1)$$

It was found that in the region of the absorption coefficient  $\alpha \geq 10^3 \text{ cm}^{-1}$  for  $Ge_2Sb_2Te_5$  films, the Tauc quadratic absorption law  $(\alpha h\nu)^{1/2} \sim (h\nu - E_g)$  is well satisfied [14,15]. The optical band gap  $E_g$  was determined from the spectral dependences of the absorption coefficient  $\alpha$  in the region corresponding to the edge of the fundamental absorption band by extrapolating the experimental dependences  $(\alpha h\nu)^{1/2} = f(h\nu)$  onto the energy axis (Fig. 5).

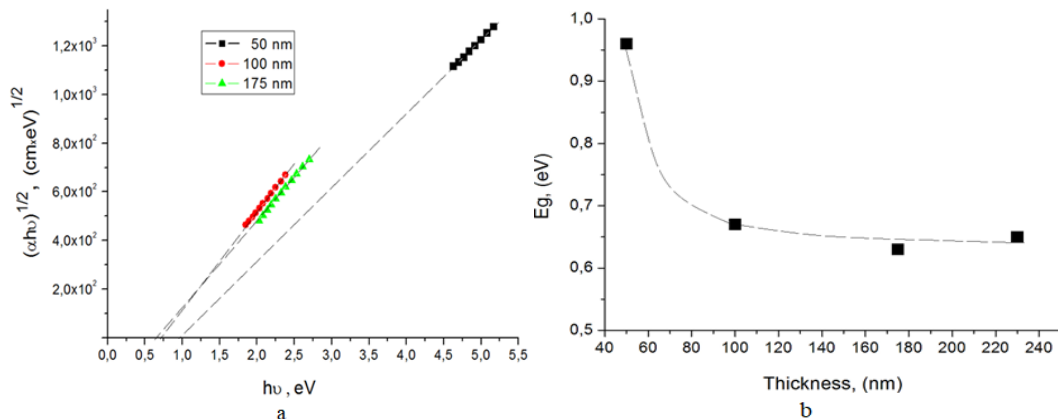


Fig. 5. Spectral dependence of the optical absorption edge (a) and the optical band gap (b) of  $Ge_2Sb_2Te_5$  films for different thicknesses.

The error in determining  $E_g$  was determined by the spread of values from sample to sample and amounted to  $\pm 0.01$  eV. The dependence of the optical band gap on the film thickness is shown in Fig. 12.

As can be seen from Fig. 5 (b), with a decrease in the thickness of the  $\text{Ge}_2\text{Sb}_2\text{Te}_5$  films from 100 to 50 nm, the optical band gap of the films increases significantly, i.e. a pronounced size effect is observed. Note that in [16], the validity of using the Tauc approach for estimating the optical band gap of nanosized films was shown. The value of  $E_g$  of nanosized  $\text{Ge}_2\text{Sb}_2\text{Te}_5$  films was determined in the range of their thicknesses from 22 to 15 nm and an increase in  $E_g$  from 2.01 to 2.09 eV was established.

The observed increase in the band gap of  $\text{Ge}_2\text{Sb}_2\text{Te}_5$  films with a decrease in their thickness from  $\sim 100$  nm is apparently associated with a decrease in the density of electronic states that form the edges of allowed energy bands (the valence band  $E_v$  and the conduction band  $E_c$ ).

### 3.4 Switching effect in $\text{Ge}_2\text{Sb}_2\text{Te}_5$

To study the switching effect, the samples were prepared in the form of "sandwich" structures. The block diagram of the measuring setup is shown in Figure 6. The bottom electrode was a continuous aluminum film deposited by thermal evaporation on a glass substrate. As the upper electrode, a point pressure contact made of gold was used, the diameter of the contact pad of which was 54.4 microns (Fig. 6).

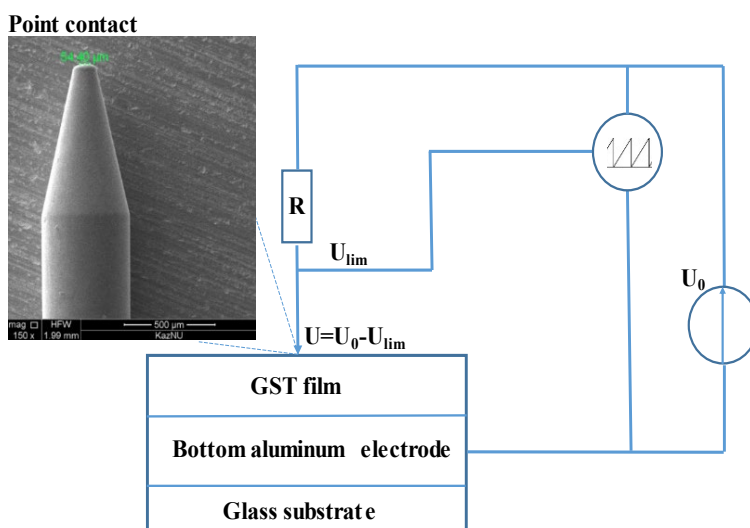


Fig. 6. Block diagram of the setup for studying the  $I$ - $V$  characteristics of films.

A sawtooth voltage with an amplitude of up to 10 V was applied to the samples from an Aktakom ANR-1011 generator. Volt-ampere characteristics recorded by the Gwinstek GDS-71062A oscilloscope. The current passing through the sample was calculated from the voltage drop across the resistor  $R_{\text{limit}}$  connected in series with the sample.

Figure 7 show experimental  $I$ - $V$  characteristics of  $\text{Ge}_2\text{Sb}_2\text{Te}_5$  films for different thicknesses. The  $I$ - $V$  characteristic has an S-shape, characteristic of the switching effect. The current-voltage characteristic shows a region of rapid current growth, which occurs during the time  $t_{\text{sw}}$  of the material switching from the high-resistance state to the conducting low-resistance state when the threshold voltage  $U_{\text{th}}$  is reached. The  $I$ - $V$  characteristics also show the values of the current in the low-resistance state  $I_{\text{on}}$ , the reverse transition current  $I_{\text{h}}$ , the transition current from the high-resistance state to the conductive state  $I_{\text{th}}$ , and the minimum reverse transition voltage  $U_{\text{h}}$ , at which the conductive state is maintained.

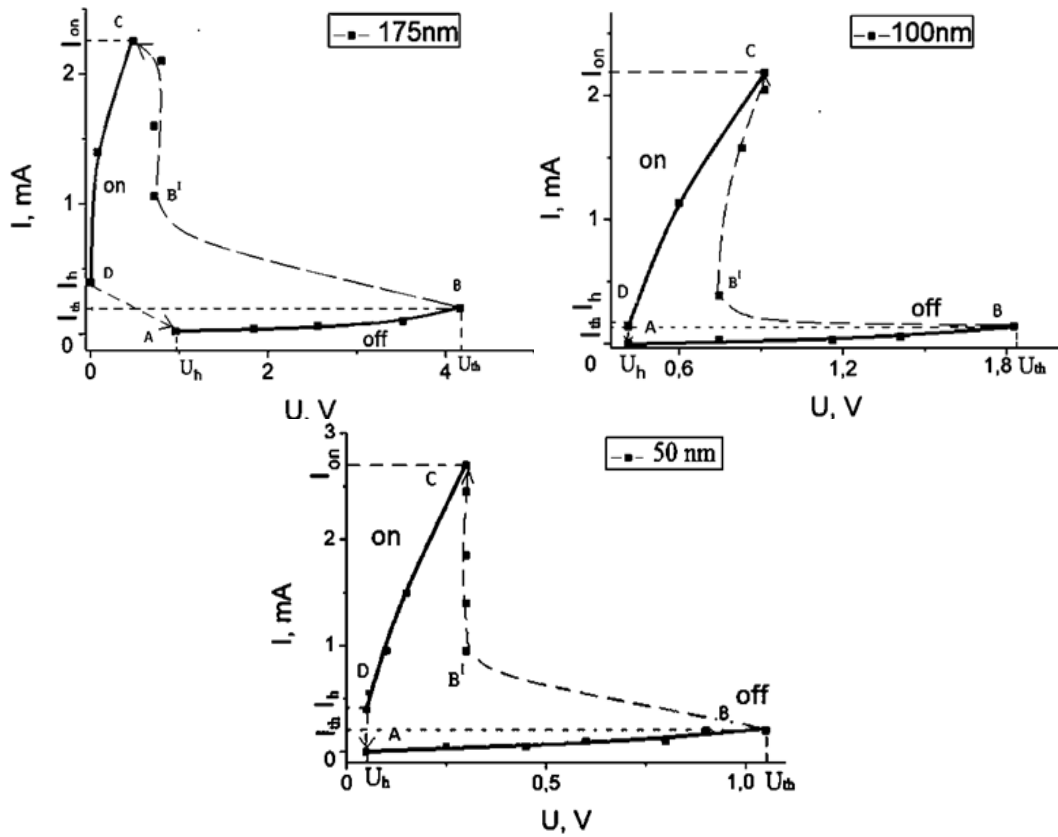


Fig. 7. Volt-ampere characteristics of  $\text{Ge}_2\text{Sb}_2\text{Te}_5$  films.

On the volt-ampere characteristics, shown in Figure 7, four specific sections can be distinguished: AB - section of the high-resistance state of  $\text{Ge}_2\text{Sb}_2\text{Te}_5$  films; BB' - section of the switching effect with the formation of a conductive cord; B'C is a section characterized by an almost constant voltage  $U_h$  with an increasing current value, depending on the thickness; CD is the section in which the low-resistance state is preserved. It is important to note that the  $U_{th}$  parameter is responsible for the formation of the conduction channel.

Table 2. Switching effect parameters.

Thickness, nm	$U_{th}$ , V	$t_{sw}$ , ns
175	4,0	100
100	1,8	70
50	1,0	50

From the analysis of the results, a significant effect of the film thickness on the parameters of the switching effect  $U_{th}$  and  $t_{sw}$  follows. Reducing the film thickness from 175 to 50 nm leads to a decrease in the threshold voltage and switching time by a factor of 4 and 2, respectively. Comparing the obtained values of the switching effect parameters for our  $\text{Ge}_2\text{Sb}_2\text{Te}_5$  films with films obtained by thermal evaporation in vacuum, for which the switching time is on the order of  $\sim 150$  ns, we can conclude that the  $\text{Ge}_2\text{Sb}_2\text{Te}_5$  films prepared by ion-plasma sputtering have lower values of the threshold switching voltage  $U_{th}$  and switching time  $t_{sw}$ . Apparently, the established improvement in the parameters of switching effects is associated with a more perfect structure of films obtained by ion-plasma sputtering.



The switching effect in CGS films, in particular, in the Ge-Sb-Te system, is due to the reversible "glass-to-crystal" phase transition. The mechanism of the switching effect is most fully explained on the basis of the electron-thermal model [5, pp. 599-607]. These works show that the switching and memory effects in CGSs are based on multiphonon tunneling ionization of U- minus centers, which, together with Joule heating, is responsible for the S-shape of the volt-ampere characteristic. The glass-crystal structural phase transition occurs in CGS due to the Joule heat increased due to the conductivity, which is sharply increased due to the multiphonon tunneling thermal ionization of intrinsic structural defects.

#### 4. Conclusion

We have developed a technique for producing thin Ge<sub>2</sub>Sb<sub>2</sub>Te<sub>5</sub> films by ion-plasma sputtering with an amorphous structure controlled by thickness and composition. The optical and electrical properties of Ge<sub>2</sub>Sb<sub>2</sub>Te<sub>5</sub> thin films have been studied and their semiconductor parameters have been determined. It is shown that the thickness of the Ge<sub>2</sub>Sb<sub>2</sub>Te<sub>5</sub> films has a significant effect on their semiconductor parameters in the thickness range from 100 to 50 nm (size effect). In this case, a correlation is observed between changes in the film thickness and changes in their optical band gap  $E_g$ . The switching effect in Ge<sub>2</sub>Sb<sub>2</sub>Te<sub>5</sub> films is studied.

#### Acknowledgments

This work is financially supported by Ministry of Science and Higher Education of the Republic of Kazakhstan under Research Project No. AP13268877 Development of manufacturing technology for radiation-resistant electronic components of artificial Earth satellites.

#### References

- [1] Kolomiets, B. T. (1964), *Physica Status Solidi B*, 7 (2): 359-372; <https://doi.org/10.1002/pssb.19640070202>
- [2] Kolomiets, B. T. (1964), *Physica Status Solidi B*, 7 (3): 713-731; <https://doi.org/10.1002/pssb.19640070302>
- [3] Ovshinsky, S. R. (1968), *Physical review letters*, 21(20), 1450; <https://doi.org/10.1103/PhysRevLett.21.1450>
- [4] Mott, N. F. (1969), *Philosophical Magazine*, 19(160), 835-852; <https://doi.org/10.1080/14786436908216338>
- [5] Bogoslovskiy, N. A., & Tsendin, K. D. (2012), *Semiconductors*, 46, 559-590; <https://doi.org/10.1134/S1063782612050065>
- [6] Kolomiets, B. T., Averianov, V. L., Liubin, V. M., & Prikhodko, O. I. (1982), *Solar Energy Materials*, 8, 1-8; [https://doi.org/10.1016/0165-1633\(82\)90044-2](https://doi.org/10.1016/0165-1633(82)90044-2)
- [7] Yamada, N., Ohno, E., Akahira, N., Nishiuchi, K. I., Nagata, K. I., & Takao, M. (1987); *Japanese Journal of Applied Physics*, 26(S4), 61; <https://doi.org/10.7567/JJAPS.26S4.61>
- [8] Krbal, M., Kolobov, A. V., Fons, P., Tominaga, J., Elliott, S. R., Hegedus, J., & Uruga, T. (2011), *Physical Review B*, 83(5), 054203; <https://doi.org/10.1103/PhysRevB.83.054203>
- [9] Kolobov, A. V., Tominaga, J., Fons, P., & Uruga, T. (2003), *Applied physics letters*, 82(3), 382-384; <https://doi.org/10.1063/1.1539926>
- [10] Shportko, K., Kremers, S., Woda, M., Lencer, D., Robertson, J., & Wuttig, M. (2008), *Nature materials*, 7(8), 653-658; <https://doi.org/10.1038/nmat2226>
- [11] Cohen, M. H., Fritzsche, H., & Ovshinsky, S. R. (1969), *Physical Review Letters*, 22(20), 1065; <https://doi.org/10.1103/PhysRevLett.22.1065>

- [12] Adler, D., Hensch, H. K., & Mott, N. (1978), *Reviews of Modern Physics*, 50(2), 209, <https://doi.org/10.1103/RevModPhys.50.209>
- [13] Kato, T., & Tanaka, K. (2005), *Japanese journal of applied physics*, 44(10R), 7340; <https://doi.org/10.1143/JJAP.44.7340>
- [14] Zakery, A., & Elliott, S. R. (2007). *Optical nonlinearities in chalcogenide glasses and their applications* (Vol. 135). Springer.
- [15] Dzhurkov, V., Fefelov, S., Arsova, D., Nesheva, D., & Kazakova, L. (2014, December), *Journal of Physics: Conference Series* (Vol. 558, No. 1, p. 012046). IOP Publishing; <https://doi.org/10.1088/1742-6596/558/1/012046>
- [16] Yao, H. B., Shi, L. P., Chong, T. C., Tan, P. K., & Miao, X. S. (2003), *Japanese journal of applied physics*, 42(2S), 828; <https://doi.org/10.1143/JJAP.42.828>